

Cite this: *RSC Adv.*, 2015, 5, 14482

# Establishment of a controlled insulin delivery system using a glucose-responsive double-layered nanogel†

DaeYong Lee,<sup>a</sup> Kibaek Choe,<sup>b</sup> YongJun Jeong,<sup>a</sup> Jisang Yoo,<sup>a</sup> Sung Mun Lee,<sup>c</sup> Ji-Ho Park,<sup>d</sup> Pilhan Kim<sup>b</sup> and Yeu-Chun Kim<sup>\*a</sup>

Glucose-responsive insulin delivery systems have been proposed as a promising alternative to conventional intramuscular administration methods, which causes low patient compliance due to the requirement of multiple administration. In addition, protein-based glucose-responsive systems using glucose oxidase and lectin have not achieved success in clinical trials because of their low biostability and potential cytotoxicity. In order to overcome these issues, the phenylboronic acid (PBA)-derivatives converted to hydrophilic moieties with an elevated glucose level play a key role in controlled insulin delivery systems due to their better biostability and high biocompatibility. In order to endow glucose-responsiveness to insulin delivery carriers using PBA derivatives, a glycol chitosan (GC)/sodium alginate (SA)-poly(L-glutamate-co-*N*-3-L-glutamylphenylboronic acid) (PGGA) graft polymer double-layered nanogel is synthesized by *N*-carboxyanhydride (NCA) polymerization and carbodiimide coupling reactions. The GC/SA-PGGA double-layered nanogel controllably releases insulin at diabetic glucose levels *in vitro*, and shows high biocompatibility, determined by cell viability and a hemolysis assay. Moreover, controlled insulin release at high glucose levels can be accomplished using the GC/SA-PGGA double-layered nanogel in mouse studies. Therefore, the GC/SA-PGGA double-layered nanogel characterized by glucose-sensitivity and superior biocompatibility may act as a potential platform for advanced insulin delivery systems.

Received 18th December 2014

Accepted 23rd January 2015

DOI: 10.1039/c4ra16656f

[www.rsc.org/advances](http://www.rsc.org/advances)

## 1. Introduction

Insulin, a peptide hormone produced by Langerhans beta cells in the pancreas, is essential to control a normal glucose level in the blood by activating the conversion of glucose to larger molecules such as glycogen and fatty acids.<sup>1</sup> Diabetic patients lose the capability of producing insulin or disorderly secrete insulin from the pancreas, caused by innate genetic defects or excessive intake of carbohydrates or fat.<sup>2</sup> For the regulation of an abnormal glucose level in the blood in diabetic patients, insulin is generally administrated by intravascular injection on a frequent basis, causing great inconvenience and low patient compliance.<sup>1,3,4</sup> In order to resolve these issues for diabetic

patients, there has been an ongoing impetus to create alternative routes of therapeutic administration that are non-invasive and convenient, such as intradermal, oral, nasal and drug delivery system.<sup>4–6</sup> However, as of yet, most of these recently devised alternative drug delivery routes have been incapable of being implemented into clinical practice due to several technological limitations.<sup>3</sup> The concept of stimuli-responsive drug delivery systems have recently gained much interest because of its distinct controlled drug release characteristic.<sup>7</sup> Such systems can respond to external stimuli, such as pH, temperature, redox-potential and glucose, by converting their chemical or physical properties, thereby establishing a framework for self-regulatory drug release.<sup>7</sup> Glucose-responsive systems have been widely used in various biomedical applications such as controlled insulin delivery and glucose concentration diagnosis.<sup>7,8</sup> The schematic architecture of currently existing glucose-responsive systems can be narrowed down to three main categories: glucose oxidase, lectin, and phenylboronic acid (PBA)-modified systems.<sup>8</sup> Glucose oxidase is an enzyme which can catalyze the oxidation process from glucose to gluconic acid.<sup>8,9</sup> Because of this characteristic, pH-sensitive polymers have been combined with glucose oxidase by conjugating glucose oxidase to the side chain or backbone of the polymer.<sup>8–10</sup> Conversion to gluconic acid lowers the pH of the solution, and

<sup>a</sup>Department of Chemical and Biomolecular Engineering, Korea Advanced Institute of Science and Technology (KAIST), Daejeon 305-701, Republic of Korea. E-mail: dohmanyi@kaist.ac.kr

<sup>b</sup>Graduate school of Nanoscience and Technology, Korea Advanced Institute of Science and Technology (KAIST), Daejeon 305-701, Republic of Korea

<sup>c</sup>Department of Biomedical Engineering, Khalifa University of Science, Technology and Research (KUSTAR), Abu Dhabi 127-788, UAE

<sup>d</sup>Department of Bio and Brain Engineering, Korea Advanced Institute of Science and Technology (KAIST), Daejeon 305-701, Republic of Korea

† Electronic supplementary information (ESI) available. See DOI: 10.1039/c4ra16656f

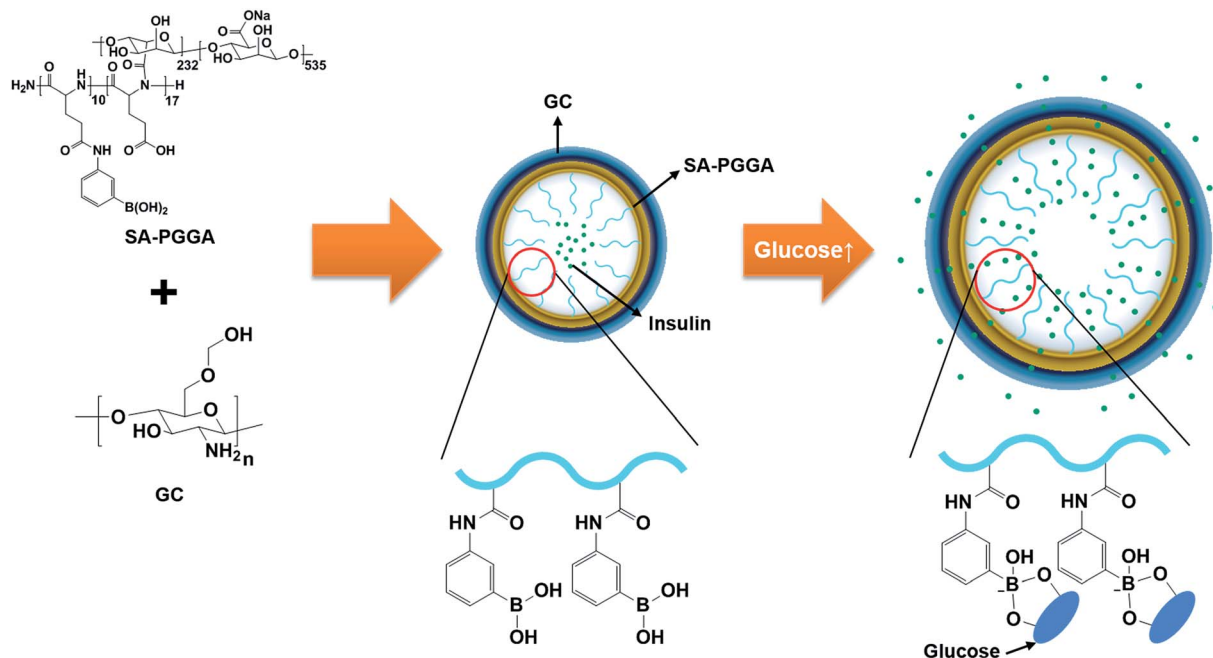


Fig. 1 Schematic illustration of glucose-responsive GC/SA-PGGA double-layered nanogel formation and controlled insulin release by complexation between PBA derivatives and glucose.

triggers swelling or deswelling of pH-sensitive groups, depending on the specific types of the groups used.<sup>8</sup> Lectins are carbohydrate-affinitive proteins, which have highly strong affinity with sugar moieties.<sup>3</sup> Concanavalin A (Con A) is a lectin protein that has four saccharide binding sites, and is strongly responsive to glucose concentration.<sup>1,11</sup> In glucose-responsive systems, Con A is generally complexed with a saccharide-modified polymer chain. The complex between Con A and saccharide can be dissociated by the replacement of free glucose, allowing release of encapsulated agents.<sup>1,11–13</sup> However, the glucose oxidase and lectin protein-based glucose responsive systems have shown many limitations in practical applications due to low biostability and relatively high toxicity.<sup>8</sup> PBA-modified glucose-responsive systems have recently gained much interest as a promising approach in that they exhibit better biostability and low toxicity compared to the other two types of glucose-responsive systems.<sup>3,6,14–21</sup> PBA and its derivatives possess strong affinity with 1,2-diol compounds, resulting in the formation of five- and six-membered rings, which is thermodynamically a favorable binding event.<sup>15</sup> In an aqueous solution, PBA is equilibrated between two forms: dehydrated and hydrated forms. With increasing glucose level, glucose molecules specifically bind to the boron of PBA, and the PBA becomes negatively ionized. Hence, the equilibrium between the two originally existing forms is broken, and the newly formed glucose–PBA complex becomes the dominant form.<sup>5,15</sup> However, PBA cannot solely endow a glucose-responsive characteristic at physiological pH, since the electron density of the boron is relatively high by the resonance effect.<sup>15</sup> Electron withdrawing group (EWG)-conjugated PBA derivatives lower the electron density of the boron, thereby enabling the PBA derivatives to have strong affinity with glucose molecules at a

physiological pH value.<sup>16</sup> Hence, EWG-conjugated PBA facilitates the conversion of the complex from a hydrophobic to hydrophilic property at physiological pH.<sup>5,15,17</sup> Herein, we propose that glycol chitosan (GC)/sodium alginate (SA)-poly(L-glutamate-co-N-3-L-glutamylphenylboronic acid) (PGGA) graft polymer double-layered nanogel can exhibit excellent bio-compatibility with potential glucose-responsive characteristic. We hypothesize that GC/SA-PGGA double-layered nanogel being glucose-responsive in nature, would enhance control release of insulin at elevated glucose levels (Fig. 1). The glucose molecules may bind to the boron atoms of the PBA derivative, and the PGGA chains can be converted to hydrophilic structures, resulting in swelling and the consequent release of insulin (Fig. 1). The endowment of this glucose-responsive characteristic was confirmed by degree of swelling and cumulative insulin release test with various glucose concentrations. The biocompatibility of GC/SA-PGGA double-layered nanogel was confirmed by cell viability assay with Henrietta Lacks (HeLa) cells. Furthermore, mouse study was conducted to demonstrate the controlled insulin release and reduced frequency of insulin administration for enhanced patient compliance. Thus, we conclude that GC/SA-PGGA double-layered nanogel may contribute to the future development of novel controlled release of insulin delivery systems with improved patient compliance.

## 2. Materials and methods

### Materials

NMR solvents, anhydrous tetrahydrofuran (THF), anhydrous dimethylformamide (DMF), hexamethyldisilazane (HMDS), sodium alginate (SA), glycol chitosan (GC), bovine pancreas

insulin, methyl thiazolyl tetrazolium (MTT), Dulbecco's Modified Eagle's Medium (DMEM), heat-inactivated fetal bovine serum, and antibiotic antimycotic solution were purchased from Sigma Aldrich. 5-Benzyl-L-glutamate and triphosgene were purchased from Alfa Aesar. 3-Aminophenylboronic acid (APBA), morpholine, fluorenylmethyloxycarbonyl (Fmoc) chloride, *N*-hydroxysuccinimide (NHS), and 1-ethyl-3-(3-dimethylaminopropyl)carbodiimide (EDC)·HCl were purchased from Tokyo Chemical Industry Co., Ltd. Precipitating and high performance liquid chromatography (HPLC) grade solvents were purchased from Daejung Chemical and Metals Co., Ltd. Molecular weight cut off (MWCO) 10 000 g mol<sup>-1</sup> dialysis bag was purchased from Spectrum Laboratories, Inc. Reduced serum medium Opti-MEM® was purchased from Gibco® by Life Technologies™.

### Characterization

GPC analysis was performed using HPLC system (YL9100, Younglin, Korea) consisting of quaternary pump, refractive index detector, adiabatic oven, vacuum degasser and 10<sup>3</sup> to 10<sup>5</sup> g mol<sup>-1</sup> DMF GPC column (KD-803, Shodex, Japan). 0.01 M LiBr DMF solution was used as a mobile phase at 35 °C with a flow rate of 1 mL min<sup>-1</sup>. A 400 MHz NMR spectrometer (400 MHz 54 mm NMR DD2, Agilent, USA) was used for <sup>1</sup>H spectra measurements. Deuterated dimethyl sulfoxide (DMSO-d<sub>6</sub>) and D<sub>2</sub>O were used as a NMR solvent. Fourier transform infrared (FT-IR) spectrometry analysis was conducted using FT-IR spectrometer (Alpha-p, Bruker, Germany). The particle size and size distribution were measured with a dynamic light scattering (DLS) method (Zetasizer nano zs, Malvern, UK) conducted with a He-Ne (633 nm) and 90° collecting optics at room temperature (RT). The samples were prepared with 1 mg mL<sup>-1</sup> concentration. An element analyzer (Flash 2000, Thermo scientific, USA) was used for element analysis of carbon, nitrogen and oxygen weight percent. The samples were prepared with 1 mg mass. TEM was conducted using 120 kV FEI Technai G2 Bio-TEM. To prepare for the TEM sample, 0.01 mg mL<sup>-1</sup> of the double-layered nanogel solution was dropped onto a 230 mesh copper grid with carbon, and then negatively stained with 2% uranyl acetate solution. The copper grid was dried by a heater within a minute.

### Poly(5-benzyl-L-glutamate) (PBLG) synthesis

5-Benzyl-L-glutamate NCA was synthesized by methods described in the previous literature.<sup>22,23</sup> In a glove box, 5-benzyl-L-glutamate NCA (4 g) was dissolved into anhydrous DMF. HMDS (63 µL) was added into the mixture. The feeding molar ratio of 5-benzyl-L-glutamate NCA to HMDS was 50.<sup>24</sup> The mixture was stirred at RT for 2 days. After polymerization, the mixture was poured into methanol. The precipitate was filtered, washed with methanol and dried at RT for overnight. PBLG (3.2 g) was obtained (yield: 96%).

### Deprotection of PBLG

PBLG (3.0 g) was suspended into deionized water. Sodium hydroxide (1.16 g) was added into the suspension. The reaction mixture was stirred at RT for 1 day. For the neutralization of

basic conditions, 35% hydrochloride solution (1 mL) was slowly added into the cloudy suspension. The suspension was stirred at RT for 30 min. It was dialyzed against deionized water for 1 day. The dialyzed suspension was lyophilized to obtain the poly-L-glutamate (PLG) (1.8 g)<sup>25</sup> (yield: 86%).

### Fmoc-protection of PLG

PLG (2.4 g) was dissolved into anhydrous DMF. Fmoc chloride (0.06 g) was added into the mixture. The reaction mixture was stirred at RT for 3 h. The mixture was precipitated with diethyl ether. The precipitate was washed with diethyl ether three times and filtered by vacuum filtration to obtain the Fmoc-protected PLG (1.8 g) (yield: 75%).

### Poly(L-glutamate-co-N-3-L-glutamylphenylboronic acid) (PGGA) synthesis

Fmoc-protected PLG (3.0 g) was dissolved into DMSO. EDC·HCl (11.0 g) and NHS (4.5 g) were added into the mixture. After 20 min, APBA (2.7 g) was added into the mixture.<sup>3</sup> The mixture was stirred at RT for 1 day. Then, the mixture was precipitated with methanol and filtered by vacuum filtration. The white brown powder was dried at reduced pressure. Fmoc-protected PGGA was dissolved into DMF. Morpholine 20% (v/v) in DMF was added into the solution. The reaction mixture was stirred at room temperature for 3 h. The reaction mixture was precipitated with diethyl ether, washed several times, and dried at reduced pressure. PGGA (3.2 g) was obtained (yield: 71%).

### SA-PGGA synthesis

SA (10 mg) was dissolved into distilled water. EDC·HCl (50 mg) and NHS (10 mg) were dissolved into the SA solution and stirred at RT for overnight. PGGA (4.4 g) was dissolved in DMSO and the PGGA DMSO solution was slowly added into the solution. The reaction mixture was stirred at 40 °C for 3 days. The reaction mixture was dialyzed (MWCO 10 000) against deionized water for 3 days. The large aggregate was filtered and the suspension was lyophilized. SA-PGGA (1 g) was obtained (yield: 3.8%).

### Insulin-loaded GC/SA-PGGA nanogel preparation

GC/SA-PGGA double-layered nanogel was prepared by an isotropic gelation method and electrostatic interactions.<sup>26</sup> SA-PGGA (10 mg) was dissolved into DI water (10 mL) and insulin solution (1 mL in 1 mg mL<sup>-1</sup> 0.01 N HCl solution) was slowly added into SA-PGGA solution while pipetting for 5 min. In order to use an isotropic gelation, calcium chloride solution (470 µL in 1.1 mg mL<sup>-1</sup> deionized water) was added in the solution and then SA-PGGA solution was mixed by pipetting for 10 min. To form GC/SA-PGGA double-layered nanogel, GC solution (1 mg mL<sup>-1</sup> in 1 mg mL<sup>-1</sup> deionized water) was slowly added into the SA-PGGA solution while pipetting for 10 min. To remove unloaded-insulin, the solution was dialyzed against deionized water for 1 day and then, lyophilized. Insulin-loaded GC/SA-PGGA double-layered nanogel (15 mg) was obtained.

### Confirmation of biocompatibility and blood compatibility

The biocompatibility of synthetic nanogels was evaluated by MTT assay using HeLa cells.<sup>6</sup> The HeLa cells were seeded in 96-well plate at 10 000 cells per one well in DMEM (100  $\mu$ L) with 10% heat-inactivated fetal bovine serum and 1% antibiotic antimycotic solution, and incubated at 37 °C in 5% CO<sub>2</sub> atmosphere. After 1 day-incubation, the medium was removed, and each well containing HeLa cells was treated with different nanogel solutions (100  $\mu$ L): SA, SA-PGGA, GC, and GC/SA-PGGA for 24 h (in reduced serum medium (90  $\mu$ L) and each nanogels in phosphate buffered saline (PBS) solution (10  $\mu$ L, 10 mg mL<sup>-1</sup> each sample dissolved in PBS)). Following 24 h of incubation with nanogel solutions, the medium was removed, and MTT solution (20  $\mu$ L, 5 mg mL<sup>-1</sup> in PBS solution) was added into each well. MTT solution-treated cells were incubated for 3 h. After that, solubilization buffer (10% triton-X in isopropanol containing 35% hydrochloride solution (2.5  $\mu$ L) was added into each well. The absorbance of each solution in each well was quantified by UV-Visible (UV-Vis) spectrometer (MultiSkan™ Go, Thermo Scientific, USA) at 590 nm. The cell viability was expressed as the ratio of absorbance with non-treated cells to absorbance with sample-treated cells. All the experiments were triplicated. The blood compatibility demonstration of nanogels was performed using hemolysis assay.<sup>3</sup> Blood was drawn from a mouse and stored in an ethylenediaminetetraacetate-treated tube. In the first step, the blood sample (0.5 mL) was centrifuged at 1200g for 10 min, and then the supernatant was discarded. In the following step, saline solution (1 mL) was added into the blood sample, and the red blood cells (RBCs) were isolated by centrifugation at 1200g for 10 min, followed by washing with saline solution twice. The isolated RBCs were diluted to saline solution (5 mL). Then, diluted RBCs suspension (0.4 mL) was added into PBS, SA, SA-PGGA, GC, GC/SA-PGGA and Triton X-100 saline solutions (0.4 mL). All the polymer sample concentrations were 4 mg mL<sup>-1</sup>, and each sample (0.1 mL) was added into saline solution (0.3 mL). PBS (0.1 mL) and Triton X-100 (0.1 mL) were independently added into each saline solution (0.3 mL). Saline and Triton X-100 were used as negative and positive controls, respectively. All the treated RBCs samples were incubated at 37 °C for 1 h, and then centrifuged at 3000g for 10 min. Each supernatant (100  $\mu$ L) was transferred into a 96-well plate. The UV-Vis absorbance of each supernatant was quantified by UV-Vis spectrometer (MultiSkan™ Go, Thermo Scientific, USA) at 540 nm. Hemolysis activity of RBCs was expressed as the percentage of UV-Vis absorbance difference between sample and negative control (PBS) over the difference between positive control (Triton X-100) and negative control. All the experiments were conducted five times.

### FITC-insulin-loaded GC/SA-PGGA double-layered nanogel preparation

FITC-insulin was prepared by the previous literature procedure.<sup>27</sup> FITC-insulin-loaded GC/SA-PGGA (10 mg) was suspended in deionized water. The nanogel suspension (1 mL, 10 mg mL<sup>-1</sup> FITC-insulin-loaded GC/SA-PGGA suspension) was

poured into five dialysis bags (MWCO 10 000 g mol<sup>-1</sup>). Each dialysis bag containing the nanogel solution was soaked in various glucose solutions (0, 1, 3, 5 and 10 mg mL<sup>-1</sup>). Each glucose solution was stirred at 150 rpm. Each insulin-released solution (100  $\mu$ L) was extracted from the corresponding glucose levels at a predetermined time point. The amount of released insulin was quantified by fluorescence spectrophotometer (RF5301-PC, Shimadzu, Japan). The degree of insulin-release was expressed as the ratio of the amount of release insulin to that of total encapsulated insulin.<sup>5</sup> All the experiments were triplicated.

### Cumulative insulin release curve with different glucose levels *in vitro*

FITC-insulin-loaded GC/SA-PGGA (10 mg) was suspended in deionized water. The nanogel suspension (1 mL, 10 mg mL<sup>-1</sup> FITC-insulin-loaded GC/SA-PGGA suspension) was poured into five dialysis bags (MWCO 10 000 g mol<sup>-1</sup>). Each dialysis bag containing the nanogel solution was soaked in various glucose solutions of 0, 1, 3, 5 and 10 mg mL<sup>-1</sup>. Each glucose solution was stirred at 150 rpm. Each insulin-released solution (100  $\mu$ L) was extracted from the corresponding glucose level at a predetermined time point. The amount of released insulin was quantified by fluorescence spectrophotometry. The degree of insulin release was expressed as the ratio of the amount of release insulin to that of total encapsulated insulin.<sup>3</sup> All the experiments were triplicated.

### *In vivo* demonstration of controlled insulin release

All the animal experimental procedures were performed under approval from the Animal Care Committee of KAIST. C57BL/6 mice aged eight weeks were used. Overnight-fasted mice were anesthetized by intramuscular injection of a mixture of Zoletil® (10 mg kg<sup>-1</sup>) and xylazine (11 mg kg<sup>-1</sup>). The level of anesthesia was continuously monitored during the experiments by using a toe pinch and maintained by intramuscular injection of half the dose of initially injected Zoletil-xylazine mixture whenever a response was observed. Glucose (0.3 g kg<sup>-1</sup>) dissolved in PBS solution (100  $\mu$ L) was administrated by retro-orbital injection at 0, 70 and 260 min. Blank GC/SA-PGGA, free insulin (0.5 IU kg<sup>-1</sup>), and insulin-loaded GC/SA, prepared by the procedure described in literature<sup>26,28</sup> (0.5 IU kg<sup>-1</sup>), and insulin-loaded GC/SA-PGGA (0.5 IU kg<sup>-1</sup>) were dissolved in PBS solution (100  $\mu$ L) each and administrated by retro-orbital injection immediately after the measurement of glucose level at 0 min. Blood samples were collected from the tail veins of mice after initial injection of glucose (0 min), immediately followed by each sample injection. Subsequently, blood samples were collected at various time points to measure the blood glucose level. The blood glucose levels were measured by a glucose meter (ACCU-CHEK Active, Roche Diagnostics GmbH, Germany). Additionally, free insulin (0.25 IU kg<sup>-1</sup>) in PBS solution (100  $\mu$ L) was administrated by retro-orbital injection twice, at 0 and 70 min. Free insulin in PBS solution (100  $\mu$ L) was injected at 0 min (0.5 IU kg<sup>-1</sup>) and 70 min (0.25 IU kg<sup>-1</sup>). Each datum was expressed as normalized glucose level, which is the ratio of blood glucose level at a



predetermined time point to that at 0 min. All the experiments were quadruplicated.

### 3. Results and discussion

#### Synthesis and characterization of SA-PGGA graft polymer

PBA derivatives, which have highly strong affinity with glucose and are converted to the negatively charged forms after a binding event, are widely used for insulin delivery systems and as glucose-measuring sensors.<sup>14–16</sup> For this reason, SA-PGGA was synthesized by NCA polymerization and carbodiimide coupling reactions. In the first step, 5-benzyl-L-glutamate NCA was controlled-polymerized by using hexamethyldisilazane (HMDS) as a living initiator (Fig. 2).<sup>24</sup> The chemical structure of poly(5-benzyl-L-glutamate) (PBLG) was characterized by <sup>1</sup>H NMR spectrometry (Fig. 3a). The molecular weight and polydispersity index of PBLG, determined by gel permeation chromatography (GPC), were 6800 g mol<sup>-1</sup> and 1.1, respectively (Fig. 3b). The benzyl groups of PBLG were deprotected by transesterification method<sup>25</sup> (Fig. 2), and the chemical structure of poly-L-glutamate (PLG) was confirmed by <sup>1</sup>H NMR spectrometry (Fig. 3a). Compared to the PBLG spectrum, the phenyl peak at 7.2 ppm and the benzyl position at 4.8 ppm disappeared after deprotection (Fig. 3a). To synthesize glucose-responsive PGGA chains, 3-aminophenylboronic acid (APBA) was conjugated to the carboxyl groups of PLG, using carbodiimide coupling reaction (Fig. 2). The chemical structure of PGGA and degree of APBA conjugation were confirmed by <sup>1</sup>H NMR spectrometry (Fig. 3). As shown in the PGGA spectrum (Fig. 3a), the peaks at 7.4 to

8.1 ppm correspond to the protons of APBA. The degree of APBA conjugation was obtained by the ratio of the protons of APBA group a to that of the methylene groups b in the side chains based on the peak integration (Fig. 3a). The modification degree was 37.5% (Fig. 3a). SA-PGGA graft polymer was synthesized by carbodiimide coupling reaction between the carboxyl groups of SA and the end amine groups of PGGA (Fig. 2). The degree of PGGA conjugation was quantified by element analysis (Fig. 3c and Table S1†). The mole fraction of PGGA chains was determined based on the amine weight percent, which indicates the weight percent of PGGA chains, the number of PGGA repeating units and the degree of APBA modifications. The mole fraction of SA segments was obtained by the ratio of the total carbon moles, excluding PGGA chains' carbon moles, to the number of carbons in one SA segment. Therefore, the degree of PGGA conjugation was expressed as the ratio of the mole fraction of PGGA chains to that of SA chains, and was approximately 30% (Fig. 3b and c). Moreover, SA-PGGA graft polymer was qualitatively determined by Fourier transform (FT)-IR spectrometry (Fig. 3d). The IR absorption at 3284 cm<sup>-1</sup> (amine groups) and the three absorption peaks at 1647, 1447 and 1232 cm<sup>-1</sup>, corresponding to the phenyl ring in APBA, implied that PGGA chains were successfully bonded to SA (Fig. 3d).

#### Optimization and characterization of SA-PGGA nanogel and GC/SA-PGGA double layered nanogel

Blank SA-PGGA nanogel was prepared by gel isotropic method.<sup>26,28</sup> To find the lowest diameter of SA-PGGA nanogel,

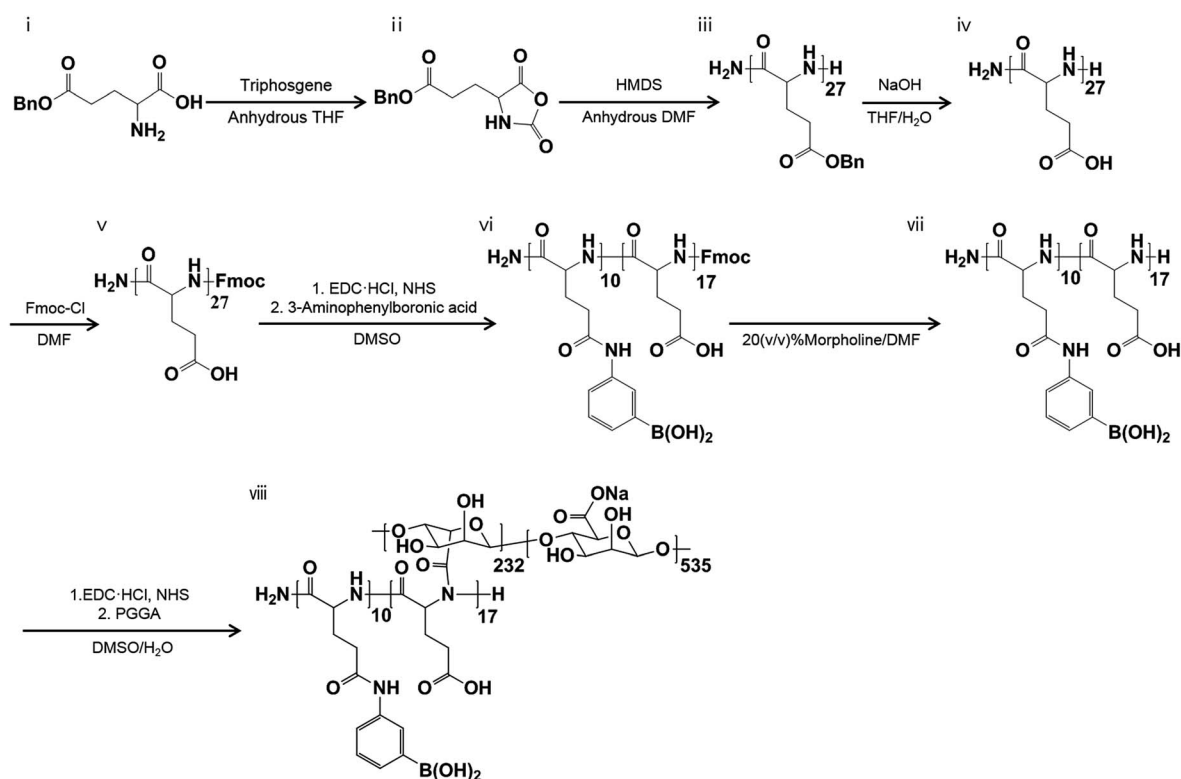


Fig. 2 Synthetic scheme of SA-PGGA graft polymer.

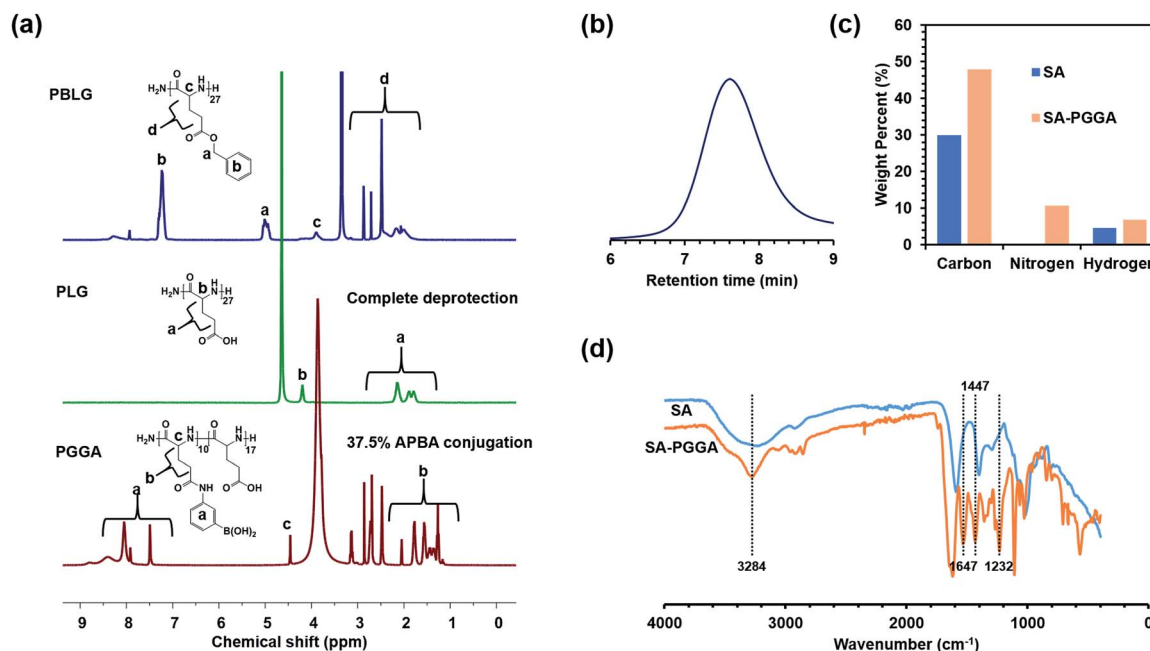


Fig. 3 (a) <sup>1</sup>H NMR spectra of PBLG (DMSO-d<sub>6</sub>), PLG (D<sub>2</sub>O) and PGGA (DMSO-d<sub>6</sub>). (b) Gel permeation chromatograph of PBLG. (c) Elemental weight ratio of SA and SA-PGGA by element analysis. (d) FT-IR spectra of SA and SA-PGGA.

SA-PGGA was treated with four different weight ratios of CaCl<sub>2</sub> (Fig. S1a†). It was found that the mean diameter of SA-PGGA nanogel was the lowest at 20 : 1 weight ratio of SA-PGGA to CaCl<sub>2</sub>. With decreasing weight ratio SA-PGGA to CaCl<sub>2</sub>, the mean diameter of SA-PGGA became increasingly higher. In addition, the zeta potential of SA-PGGA nanogel with different weight ratios of SA-PGGA to CaCl<sub>2</sub> ranged from −25 to −10 mV (Fig. S1b†). Blank GC/SA-PGGA double-layered nanogel was prepared by electrostatic interactions between the two polymers. To optimize the size of GC/SA-PGGA double-layered nanogel, SA-PGGA was treated with four different weight ratios of GC. The mean diameter of the double-layered nanogel was the lowest at 0.8 : 1 weight ratio of GC to SA-PGGA (Fig. S1c†). However, with increasing or decreasing weight ratio of GC away from this optimal point, the mean diameter of GC/SA-PGGA double-layered nanogel became progressively higher. Furthermore, the zeta-potential of GC/SA-PGGA double-layered nanogel with different ratios of GC to SA-PGGA ranged from 5 to 12 mV (Fig. S1d†). As shown in Fig. 4a, the hydrodynamic radius of insulin-loaded GC/SA-PGGA double-layered nanogel was 767.9 nm, which was much larger than that of blank GC/SA-PGGA double-layered nanogel (Fig. S1c†). The zeta-potential of insulin-loaded GC/SA-PGGA double-layered nanogel was 15 mV (Table S2†), which may be suitable for biomedical uses.<sup>7</sup> Insulin loading efficacy quantified by the insulin standard curve was 71 ± 3.5% (Table S2†). Transmission electron microscopy (TEM) measurement was employed to demonstrate the morphology and size of insulin-loaded GC/SA-PGGA double-layered nanogel. The TEM images demonstrated that the morphology was spherical (Fig. 4b). The huge difference in the nanogel diameter between DLS and TEM may be associated

with the swelling nature of GC/SA-PGGA in aqueous solution.<sup>29,30</sup>

#### Demonstration of biocompatibility of SA-PGGA and GC/SA-PGGA double layered nanogel

To demonstrate the biocompatibility of SA-PGGA nanogel and GC/SA-PGGA double-layered nanogel, methyl thiazolyl tetrazolium (MTT) assay was performed using HeLa cells.<sup>6</sup> Firstly, the cells were treated with SA, GC, blank SA-PGGA nanogel and blank GC/SA-PGGA double-layered nanogel (100 μg) for 1 day. Here, phosphate buffered saline (PBS) was used as a positive control (Fig. 5a). From MTT analysis, it was found that both SA-PGGA nanogel and GC/SA-PGGA double-layered nanogel were considerably biocompatible with the HeLa cells, exhibiting more than 80% cell viability (Fig. 5a). In the case of SA-PGGA double-layered nanogel, the biocompatibility was somewhat enhanced compared to SA (Fig. 5a). Furthermore, the fact that GC/SA-PGGA double-layered nanogel shows the highest cell viability *in vitro* confirmed that GC may allow to reduce cytotoxicity (Fig. 5b). It also observed that the GC/SA-PGGA double-layered nanogel does not affect adversely the viability of cells due to the moderate zeta-potential,<sup>7</sup> which is approximately 10 mV (Table S2†). Finally, to demonstrate the blood compatibility of GC/SA-PGGA double-layered nanogel, a blood compatibility test was performed using hemolysis activity assay.<sup>3</sup> The quantified value of hemolysis activity indicates the degree of lysed RBCs by a specific substance in contact with the blood. Therefore, a smaller percentage of hemolysis activity indicates better blood compatibility of particular substances (Fig. 5b). In this case, the hemolysis percentage of all the nanogel samples were less than 2%, even with high concentrations at 1 mg mL<sup>−1</sup>

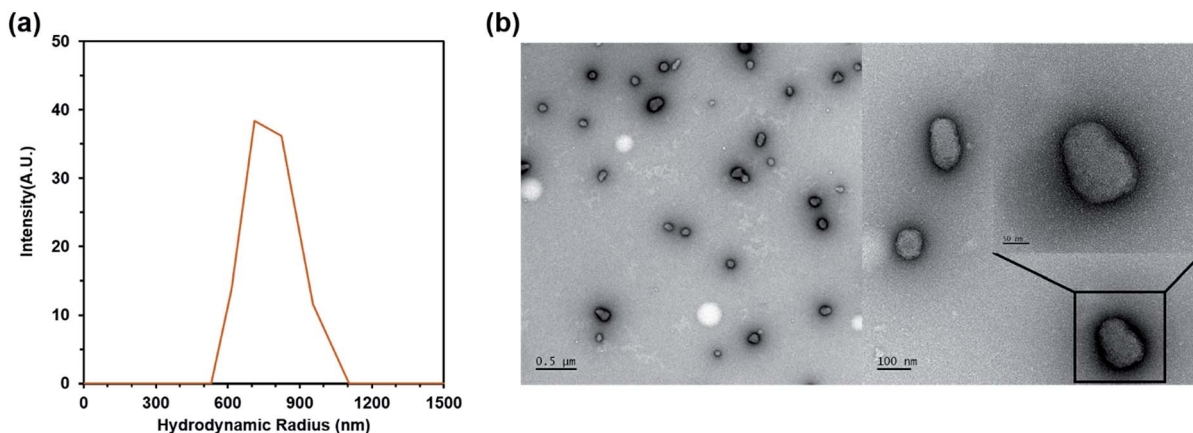


Fig. 4 (a) Hydrodynamic radius distribution of insulin-loaded GC/SA-PGGA double-layered nanogel. (b) TEM images of insulin-loaded GC/SA-PGGA double-layered nanogel.

(Fig. 5b). Therefore, based on MTT and hemolysis assay, it can be confirmed that GC/SA-PGGA double-layered nanogel is suitable for many potential biomedical applications due to its strong biocompatibility.

#### Confirmation of GC/SA-PGGA double-layered nanogel's glucose-responsive characteristic *in vitro*

To confirm the endowment of glucose-responsive characteristic, the degree of swelling and cumulative insulin release test was carried out with different glucose levels (Fig. 6a and b). We hypothesized that the hydrophobic PGGA segments conjugated to SA would be converted from hydrophobic to hydrophilic by the negative ionization of the PBA boron atom, resulting in

swelling of the nanogel.<sup>3,5,6,15</sup> GC/SA-PGGA double-layered nanogel was treated with five different glucose concentrations: 0, 1, 3, 5 and 10 mg mL<sup>-1</sup>. The degree of swelling was expressed as the ratio of the mean diameter with glucose to the mean diameter without glucose. As shown in Fig. 6a, GC/SA-PGGA double-layered nanogel was increasingly swollen with elevated glucose-concentration. At 1 mg mL<sup>-1</sup> glucose concentration, the mean diameter of GC/SA-PGGA double-layered nanogel was increased by 125% compared to the mean diameter without glucose (Fig. 6a), suggesting that a small portion of glucose molecules have bound to the boron atom of PBA derivatives.<sup>3,5,6,15</sup> At 5 mg mL<sup>-1</sup> glucose concentration, the mean diameter of GC/SA-PGGA double-layered nanogel was almost doubled over the non-treated nanogel, indicating that more

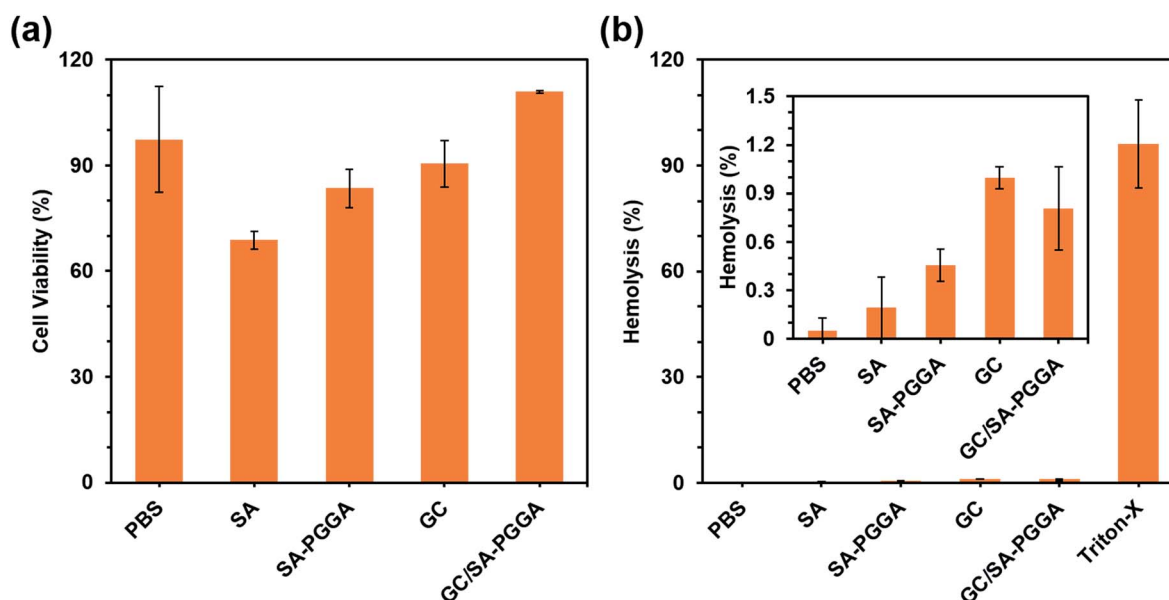


Fig. 5 (a) Determination of biocompatibility of SA, SA-PGGA, GC and GC/SA-PGGA nanogel using HeLa cell with PBS as a positive control. All the experiments were triplicated ( $n = 3$ ). The error bars were expressed as mean standard deviation. (b) Blood compatibility of SA, SA-PGGA, GC and GC/SA-PGGA using hemolysis assay with saline and Triton X-100 as negative and positive controls, respectively. All the experiments were conducted five times ( $n = 5$ ). The error bars were expressed as mean standard deviation.

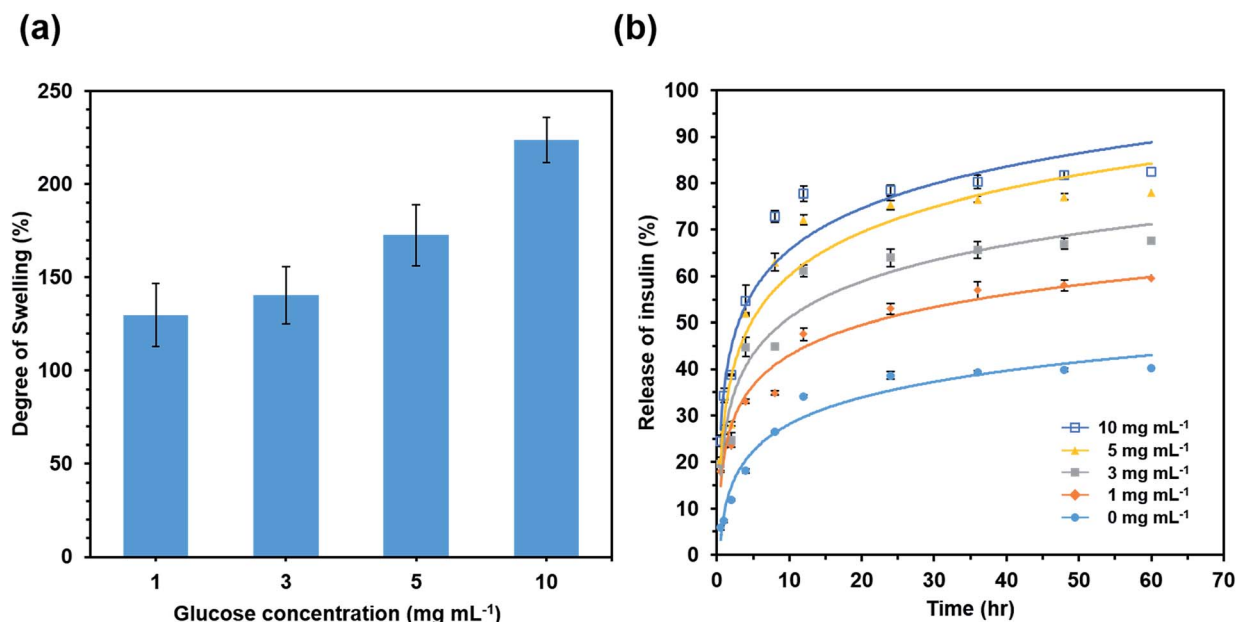


Fig. 6 (a) Determination of degree of swelling with different glucose levels (1, 3, 5 and 10 mg mL<sup>-1</sup>). (b) Cumulative insulin release curve from FITC-insulin-loaded GC/SA-PGGA double-layered nanogel in deionized water with five different glucose levels (0, 1, 3, 5 and 10 mg mL<sup>-1</sup>). All the experiments were triplicated. The error bars were expressed as mean standard deviation ( $n = 3$ ).

complexes between PBA derivatives and glucose molecules were formed.<sup>3,5,6,15</sup> Accordingly, at 10 mg mL<sup>-1</sup> glucose concentration, GC/SA-PGGA double-layered nanogel was much more swollen than the previous groups. These analysis were indicative of the excellent swelling capacity of GC/SA-PGGA double-layered nanogel with elevated glucose concentrations. Thus confirming the glucose responsive property of the double layered nanogel system. Precisely, it can be concluded that, the encapsulated insulin can be released out of core in GC/SA-PGGA double layered nanogels by swelling in response to the glucose concentration, followed by destabilization of hydrophobic moieties within the GC/SA-PGGA nanogels.<sup>15</sup> To visually demonstrate the controlled insulin release characteristic at different glucose levels, Fluorescein isothiocyanate (FITC)-insulin-loaded GC/SA-PGGA was poured into dialysis bags, and treated with five different glucose concentrations: 0, 1, 3, 5 and 10 mg mL<sup>-1</sup> in double deionized water (Fig. 6b). The resulting cumulative insulin release curve is shown in Fig. 6b. As observed higher the glucose level, the more would be the rapid release of insulin. In the case of the two high glucose levels, 5 and 10 mg mL<sup>-1</sup>, more than 50% of encapsulated FITC-insulin was rapidly released from GC/SA-PGGA double-layered nanogel until 12 h (Fig. 6b). As shown in the cumulative insulin release curves (0 and 1 mg mL<sup>-1</sup> glucose concentrations), the amount of released insulin was moderately increased until 12 h (Fig. 6b). After 1 day, most of the encapsulated insulin was released at 5 mg mL<sup>-1</sup>, a typical diabetic glucose concentration indicating that the formation of complexes between PBA derivatives and glucose molecules weakens hydrophobic interactions between PGGA segments (Fig. 6b).<sup>15</sup> On the other hand, at low glucose concentrations (0 and 1 mg mL<sup>-1</sup>), the encapsulated insulin was not released,

meaning that PGGA chains are strongly bound together by hydrophobic interaction due to incomplete complexation between PBA-derivatives and glucose molecules (Fig. 6b).<sup>15</sup> Therefore, based on the cumulative insulin release curves, it is reasonable to conclude that GC/SA-PGGA double-layered nanogel clearly exhibits a glucose-responsive characteristic and controlled release of therapeutic doses of insulin at diabetic glucose levels (3, 5 and 10 mg mL<sup>-1</sup>). Hence, we have demonstrated the potential use of GC/SA-PGGA double-layered nanogel for *in vivo* study by investigating the *in vitro* insulin release profile.

#### Demonstration of GC/SA-PGGA double-layered nanogel's controlled insulin release *in vivo*

To confirm the controlled insulin release capability of GC/SA-PGGA nanogel *in vivo*, mice were treated with four different samples: blank GC/SA-PGGA, free insulin, insulin-loaded GC/SA, and insulin-loaded GC/SA-PGGA. Blank GC/SA-PGGA and free insulin were used as negative and positive controls, respectively. Insulin-loaded GC/SA was employed as a negative comparison group to confirm the endowment of glucose-responsive characteristic on insulin-loaded GC/SA-PGGA. The dosage of insulin in each sample was 0.5 IU kg<sup>-1</sup>. Glucose was administrated to mice at 0 (all groups), 70 (excluding blank GC/SA-PGGA group) and 260 min (excluding blank GC/SA-PGGA group). Once glucose was administered to mice, their blood glucose levels immediately boosted from normal ranges to diabetic glucose ranges. Before the second glucose injection, all the blood glucose levels that of excluding blank GC/SA-PGGA followed a similar behavior in that their glucose levels were progressively lowered (Fig. 7a). Compared to



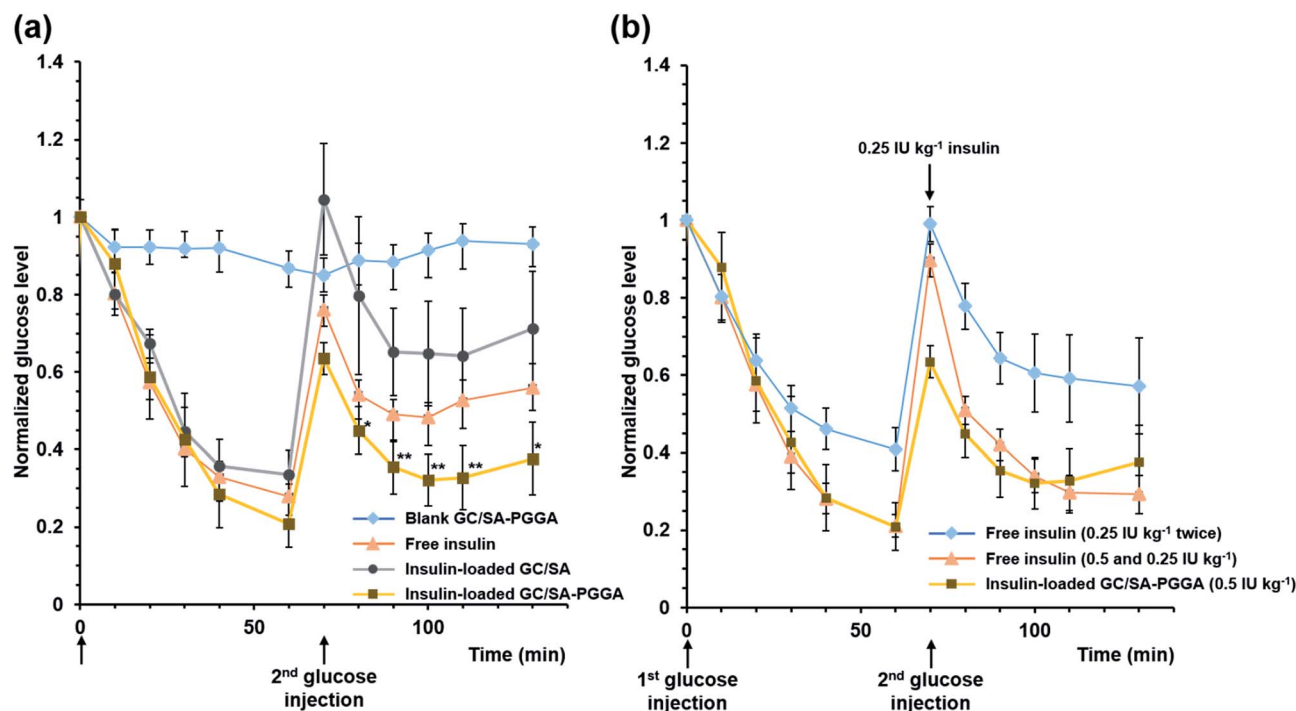


Fig. 7 (a) Normalized blood glucose levels in mice by retro-orbital administration of blank GC/SA-PGGA, free insulin, insulin-loaded GC/SA and insulin-loaded GC/SA-PGGA. (b) Normalized blood glucose levels in mice by the administration of free insulin injected twice ( $0.25 \text{ IU kg}^{-1}$ ), free insulin injected ( $0.5$  and  $0.25 \text{ IU kg}^{-1}$ ), and insulin-loaded GC/SA-PGGA ( $0.5 \text{ IU kg}^{-1}$ ). All the error bars were expressed as mean standard error ( $n = 4$ ,  $*p < 0.1$ ,  $**p < 0.05$  compared with Insulin-loaded GC/SA alone).

insulin-loaded GC/SA, insulin-loaded GC/SA-PGGA-treated mice showed that the blood glucose levels were more dramatically decreased until 60 min, meaning that GC/SA-PGGA nanogel can controllably release the encapsulated insulin by its glucose-responsiveness (Fig. 7a). After the second glucose injection, the remarkable differences in normalized glucose levels between the insulin-loaded GC/SA-PGGA group and the other group are displayed in Fig. 7a. Notably, the blood glucose levels of two particular groups, free insulin and insulin-loaded GC/SA, were no longer dramatically decreased. Moreover, the blood glucose levels were maintained, indicating that the originally administrated insulin have been nearly physiologically consumed and the insulin entrapped inside the nanogel may have stayed inside the particle core. On the other hand, the blood glucose levels were still kept relatively low, meaning that the encapsulated insulin were released more controllably (Fig. 7a). After the third glucose injection, the encapsulated insulin in the GC/SA-PGGA nanogel was almost consumed after 250 min (Table S3†). To demonstrate the reduced frequency of insulin injection, one group of mice was given two administrations of  $0.25 \text{ IU kg}^{-1}$  insulin at 0 and 70 min, and another group was treated with  $0.5$  and  $0.25 \text{ IU kg}^{-1}$  insulin at 0 and 70 min, respectively (Fig. 7b). Prior to the second glucose administration from 0 to 70 min, the blood glucose levels of free insulin ( $0.5$  and  $0.25 \text{ IU kg}^{-1}$ ), and insulin-loaded GC/SA-PGGA exhibited a similar decreasing tendency (Fig. 7b). Whereas, the blood glucose levels of mice injected twice with  $0.25 \text{ IU kg}^{-1}$  of insulin were slightly lowered compared to those of other groups

because of the difference in insulin dosage (Fig. 7b). After re-administration of  $0.25 \text{ IU kg}^{-1}$  free insulin, it was shown that the blood glucose levels of insulin-re-treated mice groups of  $0.25 \text{ IU kg}^{-1}$  free insulin resemble the plot of insulin-loaded GC/SA-PGGA from 70 min to 130 min (Fig. 7b). The similar tendency of the graphs of free insulin ( $0.5$  and  $0.25 \text{ IU kg}^{-1}$ ), and insulin-loaded GC/SA-PGGA illustrated that GC/SA-PGGA double-layered nanogel could stabilize the encapsulated insulin, and successfully achieve glucose-triggered insulin release (Fig. 7b). Consequently, a reduction in the number of insulin injection can be attained using glucose-responsive GC/SA-PGGA double-layered nanogel and contribute to the enhancement of patient compliance. Based on these results, it was found that insulin-loaded GC/SA-PGGA double-layered nanogel can controllably release the encapsulated insulin at high glucose levels and maintain low blood glucose levels for up to 3 h (Fig. 7a and b and Table S3†). Furthermore, the decreased frequency of insulin administration was demonstrated by the experimental observations as shown in Fig. 7b, followed the same behavior. Therefore, it can be concluded that GC/SA-PGGA double-layered nanogel may act as a promising platform for next generation controlled insulin release systems.

## 4. Conclusions

To conclude, we have succeeded in demonstrating the feasibility of GC/SA-PGGA double-layered nanogel as a potential controlled insulin drug delivery system. For developing this

system, initially SA-PGGA graft polymer possessing a glucose-responsive moiety was synthesized by NCA polymerization and carbodiimide coupling reactions. GC/SA-PGGA double-layered nanogel was formed by gelation method and electrostatic interactions between two polymers. The developed nanogel had size of 700 nm as per DLS, and TEM images showed much reduced size of 200 nm with a sponge-like morphology. In addition, it was found that GC/SA-PGGA double-layered nanogel showed good biocompatibility and potential hemocompatibility using MTT and hemolysis assay. In addition, they exhibited a strong glucose-responsive characteristic at diabetic glucose levels, confirmed by its degree of swelling and cumulative insulin release curve. Furthermore, we demonstrated that the insulin-loaded GC/SA-PGGA double-layered nanogel was able to controllably release the encapsulated insulin at high glucose levels *in vivo*, and maintain low glucose levels for almost 3 h. Moreover, it was confirmed that insulin-loaded GC/SA-PGGA double-layered nanogel could induce a similar blood glucose reducing effect as when free insulin was injected twice ( $0.5 \text{ IU kg}^{-1}$  and  $0.25 \text{ IU kg}^{-1}$ , and  $0.25 \text{ IU kg}^{-1}$  twice), thus demonstrating a possibility for eliminating the necessity of frequent and inconvenient insulin injections. Based on our work, we conclude that the biocompatible GC/SA-PGGA double-layered nanogel with self-regulating glucose-recognition insulin release characteristic may act as a potential platform for next generation controlled insulin delivery systems.

## Acknowledgements

This study was supported by the KUSTAR-KAIST Institute at KAIST, a grant of the Korean Health Technology R&D Project, Ministry of Health & Welfare, Republic of Korea. (Project number: HI13C0826) and Ministry of Science, ICT, and Future Planning (Project no. NRF-2014M3A9E4064580). We thank Korea Basic Science Institute (KBSI) for transmission electron microscopy facility.

## Notes and references

- 1 M. Brownlee and A. Cerami, *Diabetologia*, 1980, **19**, 261.
- 2 K. Chaturvedi, K. Ganguly, M. N. Nadagouda and T. M. Aminabhavi, *J. Controlled Release*, 2013, **165**, 129–138.
- 3 L. Zhao, J. X. Ding, C. S. Xiao, P. He, Z. H. Tang, X. Pang, X. L. Zhuang and X. S. Chen, *J. Mater. Chem.*, 2012, **22**, 12319–12328.
- 4 Y. C. Kim, J. H. Park and M. R. Prausnitz, *Adv. Drug Delivery Rev.*, 2012, **64**, 1547–1568.
- 5 L. Zhao, C. S. Xiao, J. X. Ding, P. He, Z. H. Tang, X. Pang, X. L. Zhuang and X. S. Chen, *Acta Biomater.*, 2013, **9**, 6535–6543.
- 6 G. Liu, R. J. Ma, J. Ren, Z. Li, H. X. Zhang, Z. K. Zhang, Y. L. An and L. Q. Shi, *Soft Matter*, 2013, **9**, 1636–1644.
- 7 E. Fleige, M. A. Quadir and R. Haag, *Adv. Drug Delivery Rev.*, 2012, **64**, 866–884.
- 8 Q. Wu, L. Wang, H. J. Yu, J. J. Wang and Z. F. Chen, *Chem. Rev.*, 2011, **111**, 7855–7875.
- 9 Z. Gu, T. T. Dang, M. L. Ma, B. C. Tang, H. Cheng, S. Jiang, Y. Z. Dong, Y. L. Zhang and D. G. Anderson, *ACS Nano*, 2013, **7**, 6758–6766.
- 10 W. Tai, R. Mo, J. Di, V. Subramanian, X. Gu, J. B. Buse and Z. Gu, *Biomacromolecules*, 2014, **15**, 3495–3502.
- 11 S. Tanna, M. J. Taylor, T. S. Sahota and K. Sawicka, *Biomaterials*, 2006, **27**, 1586–1597.
- 12 S. Tanna, T. S. Sahota, K. Sawicka and M. J. Taylor, *Biomaterials*, 2006, **27**, 4498–4507.
- 13 Y. N. Wang, Y. Kotsuchibashi, K. Uto, M. Ebara, T. Aoyagi, Y. Liu and R. Narain, *Biomater. Sci.*, 2015, **3**, 152–162.
- 14 K. T. Kim, J. J. L. M. Cornelissen, R. J. M. Nolte and J. C. M. van Hest, *Adv. Mater.*, 2009, **21**, 2787–2791.
- 15 T. Hoare and R. Pelton, *Biomacromolecules*, 2008, **9**, 733–740.
- 16 H. Kim, Y. J. Kang, S. Kang and K. T. Kim, *J. Am. Chem. Soc.*, 2012, **134**, 4030–4033.
- 17 D. Shiino, Y. Murata, A. Kubo, Y. J. Kim, K. Kataoka, Y. Koyama, A. Kikuchi, M. Yokoyama, Y. Sakurai and T. Okano, *J. Controlled Release*, 1995, **37**, 269–276.
- 18 M. M. Zhou, J. D. Xie, S. T. Yan, X. M. Jiang, T. Ye and W. T. Wu, *Macromolecules*, 2014, **47**, 6055–6066.
- 19 Y. Yao, H. Y. Shen, G. H. Zhang, J. Yang and X. Jin, *J. Colloid Interface Sci.*, 2014, **431**, 216–222.
- 20 T. Ye, X. M. Jiang, W. T. Xu, M. M. Zhou, Y. M. Hu and W. T. Wu, *Polym. Chem.*, 2014, **5**, 2352–2362.
- 21 R. J. Ma and L. Q. Shi, *Polym. Chem.*, 2014, **5**, 1503–1518.
- 22 J. R. Hernandez and H. A. Klok, *J. Polym. Sci., Part A: Polym. Chem.*, 2003, **41**, 1167–1187.
- 23 D. S. Poche, M. J. Moore and J. L. Bowles, *Synth. Commun.*, 1999, **29**, 843–854.
- 24 H. Lu and J. J. Cheng, *J. Am. Chem. Soc.*, 2007, **129**, 14114–14115.
- 25 W. Agut, A. Brulet, D. Taton and S. Lecommandoux, *Langmuir*, 2007, **23**, 11526–11533.
- 26 B. Sarmento, A. J. Ribeiro, F. Veiga, D. C. Ferreira and R. J. Neufeld, *J. Nanosci. Nanotechnol.*, 2007, **7**, 2833–2841.
- 27 E. Gok and S. Olgaz, *J. Fluoresc.*, 2004, **14**, 203–206.
- 28 B. Sarmento, D. Ferreira, F. Veiga and A. Ribeiro, *Carbohydr. Polym.*, 2006, **66**, 1–7.
- 29 K. Baysal, A. Z. Aroguz, Z. Adiguzel and B. M. Baysal, *Int. J. Biol. Macromol.*, 2013, **59**, 342–348.
- 30 S. B. Hua and A. Q. Wang, *Carbohydr. Polym.*, 2009, **75**, 79–84.